Magnetic ordering in synthetic oligonucleotides. A deuterium nuclear magnetic resonance investigation

Todd M. Alam and Gary Drobny

Citation: The Journal of Chemical Physics **92**, 6840 (1990); doi: 10.1063/1.458270
View online: http://dx.doi.org/10.1063/1.458270
View Table of Contents: http://scitation.aip.org/content/aip/journal/jcp/92/11?ver=pdfcov
Published by the AIP Publishing

Articles you may be interested in

Template induced chiral ordering in nematic liquid crystalline materials: A deuterium nuclear magnetic resonance study
J. Appl. Phys. **99**, 116105 (2006); 10.1063/1.2200882

Molecular weight dependence of segmental alignment in a sheared polymer melt: A deuterium nuclear magnetic resonance investigation
J. Chem. Phys. **116**, 10020 (2002); 10.1063/1.1474577

A deuterium nuclear magnetic resonance investigation of orientational order and director kinetics in aramid solutions
J. Chem. Phys. **101**, 3255 (1994); 10.1063/1.467573

Orientational order in liquid crystal solutions of polyhexylisocyanate. II. Deuterium nuclear magnetic resonance
J. Chem. Phys. **99**, 7449 (1993); 10.1063/1.465726

Nuclear magnetic resonance study of deuterium gas
J. Chem. Phys. **98**, 6154 (1993); 10.1063/1.464854

This article is copyrighted as indicated in the article. Reuse of AIP content is subject to the terms at: http://scitation.aip.org/termsconditions. Downloaded to IP: 199.212.66.33 On: Thu, 27 Nov 2014 12:31:48

Magnetic ordering in synthetic oligonucleotides. A deuterium nuclear magnetic resonance investigation

Todd M. Alam and Gary Drobny
Department of Chemistry, University of Washington, Seattle, Washington 98195

(Received 2 November 1989; accepted 2 January 1990)

Deuterium NMR of the [methyl ^{2}H]-2′-deoxythymidine labeled synthetic oligonucleotide, [d(CGCGAAT*T*CGCG)]$_2$ in a liquid crystal phase are reported. This ordered phase was observed for hydrated samples with DNA concentrations ranging from 490 to 722 mg ml^{-1}. Temperature variation of line shape and quadrupolar echo decay times were investigated, allowing the degree of alignment and changes in dynamics to be determined. At greatly reduced temperatures a cylindrical line shape was observed, as is expected for samples with the DNA helix axis aligned perpendicular to the magnetic field, while at ambient temperatures, motion about the helix axis averages this cylindrical line shape. NMR investigations at magnetic field strengths of 11.7, 9.4, and 4.7 T resulted in only minor variation in the degree of alignment.

I. INTRODUCTION

Liquid crystalline behavior of concentrated nucleic acid solutions was reported nearly three decades ago by Robinson,[1] and Luzzati *et al.*[2] This cholesteric phase has been investigated using x-ray diffraction and optical techniques,[3–9] while the phase behavior of shorter fragment (146 base pairs) has been studied using optical microscopy, ^{31}P and ^{13}C NMR.[10–13] Magnetic alignment of nucleic acids has been reported for both RNA samples[5–7] and DNA fragments.[13,14] These investigations reveal that concentrated nucleic acid solutions order with the helix axis perpendicular to the magnetic field. Recent investigation into the lyomesophases formed from the dinucleoside phosphate, d[GG] also reveals a liquid crystalline phase which aligns in magnetic fields.[15,16]

In this study ^{2}H NMR was utilized to investigate the liquid crystalline phase formed in highly hydrated samples of the [methyl ^{2}H]-2′-deoxythymidine labeled synthetic DNA dodecamer, [d(CGCGAAT*T*CGCG)]$_2$. Quadrupolar echo line shapes, spin lattice relaxation times (T_1), and quadrupolar echo decay times (T_{2e}) of the oligonucleotide were investigated over a concentration range of 722 to 277 mg ml^{-1}. Temperature and magnetic field strength effects on the liquid crystal phase were also investigated. These studies allow the development of a motional model describing the dynamics in the dodecamer, and the degree of magnetic ordering. The observation of an ordered phase opens up interesting prospects for a detailed solid-state investigation of structure and dynamics in synthetic oligonucleotides.

II. EXPERIMENTAL

For an isolated deuteron in a solid, the NMR frequency is given by

$$\omega = \omega_0 \pm \omega_Q,$$

where the angular dependent frequencies are obtained from first-order perturbation theory as

$$\omega_Q = 3\pi/4 \left(\frac{e^2qQ}{h}\right)[3\cos^2\Theta - 1 - \eta\sin^2\Theta\cos 2\Phi],$$

where (e^2qQ/h) is the quadrupolar coupling constant (QCC), and η is the asymmetry parameter describing deviation from cylindrical symmetry of the electrical field gradient (EFG) tensor about the q_{zz} axis in the principal axis system (PAS). The polar angles Θ and Φ describe the orientation of the magnetic field $\mathbf{B}_0$ in the PAS of the EFG tensor. Molecular motion can average this tensorial interaction resulting in variation of the ^{2}H NMR line shape. If the molecular motion is rapid on the time scale of ω_Q^{-1} the resonance frequencies can be defined using QCC_{eff} and η_{eff}, the effective quadrupolar coupling constant and asymmetry parameter of the averaged electrical field gradient, respectively. If the molecular motion occurs within the intermediate exchange region ($\sim\omega_Q^{-1}$), it becomes necessary to calculate the modulation effect of these molecular motions on the angular dependent frequencies. For short pulses use of exchange modifed Bloch equations allow line shapes to be determined for various motional models. The equation of motion for the complex transverse magnetization vector, $\sigma_\pm$ is given by

$$d\sigma_\pm/dt = [i\Omega_\pm + R]\sigma_\pm,$$

where $\sigma_\pm$ correspond to the single transition raising operators $[I_x(12) + iI_y(12)]$ or $[I_x(23) + iI_y(23)]$, where $|-1\rangle = |1\rangle, |0\rangle = |2\rangle$, and $|+1\rangle = |3\rangle$ are the eigenstates of an isolated deuteron. The frequency domain spectra for the two transitions are mirror images, requiring calculation of only one transition. The term $\Omega_\pm$ is a diagonal matrix containing the Larmor precession frequencies ω_Q, while the operator R describes the dynamics. Continuous dynamics may utilize the diffusion operator $R = D\nabla^2$, which is solved by expansion of $\sigma_\pm$ into a complete set of eigenfunctions and has been applied previously.[17–22] Discrete dynamics utilize a jump kinetic matrix, R_{ij} where the off-diagonal elements represent the jump rate from site i to site j, this approach has been discussed in detail.[23–25] Deuterium NMR simulations were obtained using the program MXQET[24] which can accommodate multiaxis, multisite models including corrections for finite pulse power, exchange during the pulse, and

 0021-9606/90/116840-07$03.00 © 1990 American Institute of Physics

This article is copyrighted as indicated in the article. Reuse of AIP content is subject to the terms at: http://scitation.aip.org/termsconditions. Downloaded to IP: 199.212.66.33 On: Thu, 27 Nov 2014 12:31:48

virtual FID contributions. A modified version, GNMXQET allowing different distributions of the helix axis orientation was used to simulate the aligned spectra. Static values of the quadrupole coupling constant (e^2qQ/h) and the asymmetry parameter (η) were obtained from previous monomer investigations.[26] Effective values of the quadrupole coupling constant (QCC_{eff}) and asymmetry parameter (η_{eff}) were determined from the observed line shapes assuming no motional model. All simulations were run on either a DEC Vaxstation 3200 or a Convex C1.

Solid-state ^{2}H experiments were performed at 76.75 MHz (11.7 T), 61.41 MHz (9.4 T), and 30.70 MHz (4.7 T) on home-built consoles controlled by a DEC μVaxII.[27] An eight-step phase cycled quadrupolar echo sequence,[28] $\pi/2_x - \tau_1 - \pi/2_{\pm y} - \tau_2 -$ acq, with $\pi/2$ pulse lengths less than 3 μs was used to obtain spectra. Pulse spacing, τ_1 was varied from 40 to 200 μs, with data acquisition initiated prior to the quadrupole echo by adjustment of τ_2. Spectra were obtained using 8000 to 24 000 acquisitions at the higher field and 16 000 acquisitions at the lower field. The FIDs were left shifted to the echo maximum prior to Fourier transformation. A Lorentzian line broadening of 500 to 1000 Hz was applied to the FIDs prior to transformation to obtain adequate signal to noise. Low temperature investigations were obtained using liquid-nitrogen boil-off, and were stable within $\pm$ 1 °C. Spin lattice relaxation times, T_1 were determined using an inversion recovery pulse sequence. The magnetization recovery that was determined from the echo height maximum will be referred to as a "powder average" and denoted as $\langle T_1 \rangle$. The powder average loss of phase memory as a function of pulse spacing τ_1, was determined from echo height and is denoted as $\langle T_{2e} \rangle$.

Synthesis of [methyl ^{2}H]-2′-deoxythymidine and preparation of the labeled oligonucleotide, [d(CGCGAAT*T*CGCG)]$_2$ has been described in detail previously.[26,29] To the purified, desalted DNA was added 10% NaCl by weight, followed by lyophilization from ^{2}H depleted water. The methyl labeled DNA, total weight 56.5 mgs, was packed into a 5×15 mm NMR tube. The sample was hydrated over appropriate salt solutions containing ^{2}H depleted water.[30] Equilibration of three to four weeks at each humidity level allowed for complete and uniform humidifcation. Water adsorption was monitored gravimetrically, a blank tare being used to determine and correct for water adsorption on glass. The degree of water adsorption was observed to vary at these higher hydration levels,[29] often resulting in different water content for a given relative humidity. Water content W(mol H_2O/mol nucleotide) for the dodecamer are presented in Table I.

III. EXPERIMENTAL RESULTS

The deuterium NMR spectra of the powder [methyl ^{2}H]-2′-deoxythymidine labeled dodecamer, [d(CGCGAAT*T*CGCG]$_2$ at various humidities has previously been reported.[29] Above W~25 the samples produced spectra characteristic of an aligned phase. Effective quadrupolar coupling constants QCC_{eff}, effective asymmetry parameters η_{eff}. relative intensities (RI), $\langle T_1 \rangle$, and $\langle T_{2e} \rangle$ for these elevated humidities are presented in Table I. The line shape undergoes a reduction in QCC_{eff} with increasing hydration levels. Beginning at 92% RH (W = 26.6) with a QCC_{eff} of 20.5 kHz, a 0.5 kHz reduction is observed at (W = 29.6) followed by a reduction to 15.0 KHz at 95% RH (W = 39.8). At 98% RH (W = 69.9) only a central isotropic component was observed. Characteristic spectra for a range of hydration levels are presented in Figs. 1(a)–(c). Variation of alignment with magnetic field strength was not observed, the line shape remaining virtually unchanged for 92% RH (W = 29.6) obtained at 9.4 and 4.7 T, an example being presented in Fig. 1(d).

The aligned phase at 92% RH (W = 29.6) was investigated as a function of temperature, characteristic line shapes being presented in Fig. 2. Temperature variation of QCC_{eff}, RI, and $\langle T_{2e} \rangle$ are given in Table II. With decreasing temperature QCC_{eff} changed gradually from 15.0 kHz at 309 K to 21.0 kHz at 254 K, [see Figs. 2(a)–(c)] followed by the abrupt change to a QCC_{eff} of 51.5 kHz at 228 K. At 244 K a complex intermediate line shape is observed, followed by a cylindrical line shape at 228 K [Fig. 2(d)]. A cylindrical line shape is expected for a sample where the DNA helix axis is aligned perpendicular to the magnetic field. In B-form DNA the base plane, and therefore the C_3 symmetry axis of the methyl group are oriented approximately 90° to the helix axis. When the sample was frozen in the magnet and then rotated 90° in the coil the distinct cylindrical powder pattern disappeared. Freezing the sample outside the magnet resulted in a normal powder pattern distribution.

Increasing the level of hydration from 92% RH (W = 26.6) produced a maximum in the relative intensity RI at (W = 29.6) followed by a decrese at 95% RH (W = 39.8). Variation in RI with temperature for (W = 29.6) was rather complex with several changes in

TABLE I. Line shape parameters and relaxation rates of [d(CGCGAAT*T*CGCG]$_2$[a].

RH%	W	RI	QCC_{eff} (kHz)	η_{eff}	$\langle T_1 \rangle$ (ms)	$\langle T_{2e} \rangle$ (μs)	$\langle T_{2e} \rangle$ (μs)[b]
92	26.6	0.62	20.5 ± .5	~0	146 ± 07	200 ± 18	218
92	29.6	0.79	20.0 ± .5	~0	127 ± 06	230 ± 20	213
95	39.8	0.60	15.0 ± .5	~0	103 ± 06	249 ± 24	256
98	69.9	···	~0[c]	~0[c]	···	···	

[a] Experiments performed at 298 K.
[b] Calculated value.
[c] Observed only isotropic component.

This article is copyrighted as indicated in the article. Reuse of AIP content is subject to the terms at: http://scitation.aip.org/termsconditions. Downloaded to IP: 199.212.66.33 On: Thu, 27 Nov 2014 12:31:48

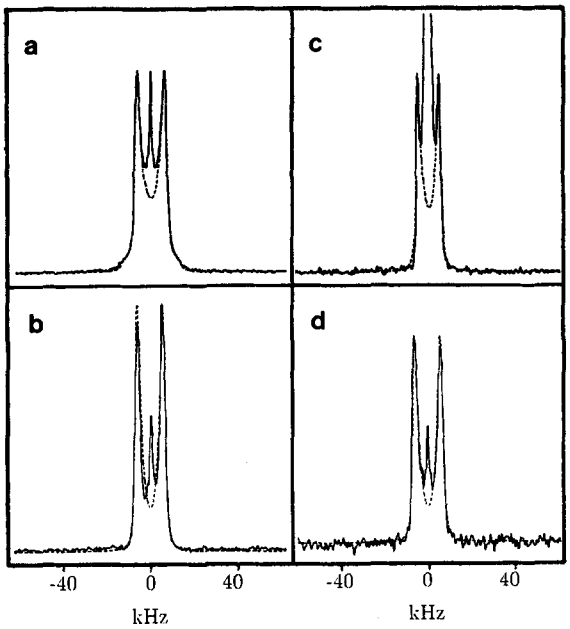

FIG. 1. Experimental and simulated (---) 76.75 MHz deuterium quadrupole echo spectra of [methyl ^{2}H]-2'-deoxythymidine labeled [d(CGCGAAT*T*CGCG)]$_2$ at various hydration levels W (mol H_2O/mol nucleotide). The simulated spectra were calculated as described in the text, ignoring the central isotropic component. Spectra for pulse delay of 50 μs at (a) 92% RH, W = 26.6, 24 000 scans, (b) 92% RH, W = 29.6, 8000 scans, (c) 95% RH, W = 39.8, 8000 scans, (d) same as (b), except at 30.70 MHz, 16 000 scans.

trends. (See Table II.) Increasing humidity above 92% RH (W = 26.6) resulted in only a small increase in the observed $\langle T_{2e}\rangle$. Variation in temperature from 309 to 244 K resulted in a decrease in $\langle T_{2e}\rangle$ by almost threefold, followed by an abrupt threefold increase in $\langle T_{2e}\rangle$ on decreasing the temperature to 228 K. Anisotropic T_{2e} effects were not readily apparent in this liquid crystalline phase. Spin lattice relaxation times, $\langle T_1\rangle$ decreased by 30% on going from 92% RH (W = 26.6) to 95% RH (W = 39.8), but these changes were small compared to the reduction in $\langle T_1\rangle$ observed for the lower hydration levels of the dodecamer.[29] Spin lattice relaxation was not investigated as a function of temperature.

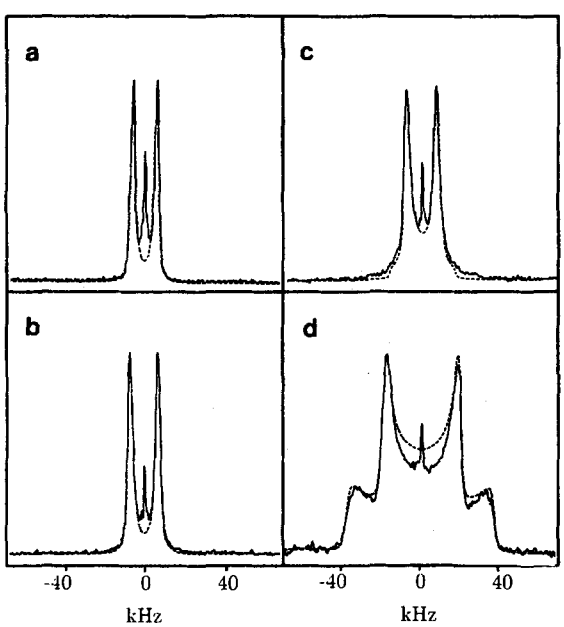

FIG. 2. Experimental and simulated (---) 76.75 MHz deuterium quadrupole echo spectrum of [d(CGCGAAT*T*CGCG)]$_2$ at 92% RH (W = 29.6) for various temperatures and 8000 scans (a) 309 K, (b) 276 K, (c) 254 K, and (d) 228 K. Simulated spectra were obtained as described in text, ignoring the central isotropic component.

TABLE II. Line shape parameters and $\langle T_{2e}\rangle$ rates of [d(CGCGAAT*T*CGCG)]$_2$[a].

Temp.(K)	RI[b]	QCC_{eff}(kHz)	$\langle T_{2e}\rangle$(μs)	$\langle T_{2e}\rangle$(μs)[c]	RI[c]
228	0.96	51.5 ± .5	324 ± 34	335	0.98
244	0.64	...	101 ± 10	...	...
254	0.68	21.0 ± .5	128 ± 12	164	0.68
276	0.83	20.5 ± .5	180 ± 16	191	0.78
286	0.84	20.5 ± .5	204 ± 18	213	0.78
295	0.79	20.5 ± .5	230 ± 20	213	0.78
309	0.76	15.5 ± .5	271 ± 30	287	0.91

[a] Experiments performed at W = 29.6 as a function of temperature.
[b] Relative echo intensity with respect to dry lyophilized powder.
[c] Calculated value.

IV. DISCUSSION

The most prominent line shape feature observed that was characteristic of an oriented phase was the reduction in shoulders intensity in the motionally averaged spectra, together with the appearance of a cylindrical line shape at reduced temperatures. Simulations of the observed data were obtained with appropriate weighting of β, which is the angle between the helix axis and the magnetic field. The spectral line shape, $I(\omega)$ can be considered a superposition of various β orientations characterized by the weighting function $f(\beta)$[18]:

$$I(\omega) = \int I(\omega,\beta) f(\beta) \sin(\beta)\, d\beta.$$

Different forms $f(\beta)$ are available, but the experimental spectra were simulated by superimposing domains where the helix axis is randomly oriented together with domains where the helix axis is highly ordered. The ordered domains were simulated by either a square well potential or a Gaussian distribution. It was found that the square well gave the inner wings that have been noted in previous liquid crystal and DNA fiber studies[18,31] as well as producing distinct cylindrical line shapes. A Gaussian distribution gave an improved fit to experimental spectra, and was assumed in all later simulations.

The functional form of $f(\beta)$ is given by

$$f(\beta) = (P/\sigma\sqrt{2\pi}) e^{-(\beta-\beta_0)^2/2\sigma^2} + (1-P),$$

where P is the fraction of the sample in oriented domains, β_0 is the mean angle of alignment, and σ is the standard variance in the Gaussian distribution. Changes in these distribution parameters produce definite variations in line shape, especially for the nonmotionally averaged cylindrical patterns of the oriented phase. Changes in the simulated line shapes for different values of P and σ, at $\beta_0 = 90°$ are shown in Figs. 3(a) and 3(b). Variation in σ alters the intensity of

This article is copyrighted as indicated in the article. Reuse of AIP content is subject to the terms at: http://scitation.aip.org/termsconditions. Downloaded to IP: 199.212.66.33 On: Thu, 27 Nov 2014 12:31:48

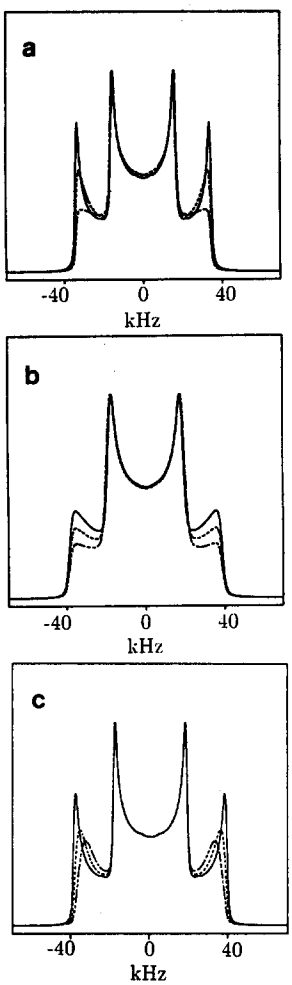

FIG. 3. Simulated quadrupole echo spectrum as a function of Gaussian distribution parameters. (a) variation in σ, (—) 1°, (---) 10°, (----) 20°, $\beta_0 = 90°$, $P = 1.0$, (b) variation in P, (—) 1.00, (---) 0.75, (----) 0.50, $\beta_0 = 90°$, $\sigma = 15°$, (c) variation in β_0, (—) 90°, (---) 80°, (----) 75°, $P = 1.0$, $\sigma = 5°$.

the parallel shoulders in the cylindrical line shape, while variation in P alters the relative intensity between the parallel shoulders and perpendicular peaks. As seen in Fig. 3(c) small deviations of the mean angle of alignment from $\beta_0 = 90°$, effectively increases the disorder σ. For orientations where $2° < |\beta_0 - 90°| < 8°$ this increase in the standard deviation can be determined from the relationship

$$\sigma(\beta_0) \approx \sigma(90°) + 1° - |\beta_0 - 90°|/2.$$

For larger differences in orientation the splitting of the outer horns changes, with no effect on the perpendicular horns. It should also be noted that a distribution in θ, which is the angle that describes the base orientation with respect to the helix axis will produce spectra that are indistinguishable from spectra with a distribution in β. The dependence of the spectral line shape on distributions in both β and θ has been thoroughly discussed by Brandes and co-workers.[31] In the analysis of experimental spectra the standard deviation σ was obtained assuming that θ and β_0 were both equal to 90°, with no distribution of θ. Analysis of x-ray crystal structure[32] and the recent NMR solution structure[33] of the oligonucleotide [d(CGCGAAT*T*CGCG)]$_2$ reveal that the base pairs indeed have a distribution of θ. The oriented oligonucleotide most likely contains distributions in both θ and β, but allowing all the distribution to appear in β the standard deviation, σ is equivalent to total standard deviation ($\sigma^2 = \sigma_\beta^2 + \sigma_\theta^2$).

Simulation of the line shape observed at 92% RH (W = 26.6) and (W = 29.6) along with 95% RH (W = 39.9) can be obtained in a similar manner as described for the study of hydration of unoriented oligonucleotides,[29] except that the degree of alignment and the percentage of random domains must be considered. These were obtained using the Gaussian orientational weighting function discussed above. The effects of helix diffusion were simulated using a jump model previously utilized in the analysis of ^{2}H and ^{31}P line shapes[34–36] on DNA as well as [methyl ^{2}H]-2′-deoxythymidine labeled [d(CGCGAAT*T*CGCG)]$_2$ at lower hydration levels. This jump model is described by the equilibrium

$$S_1 \overset{k}{\rightleftarrows} S_2 \overset{k}{\leftrightarrows} \cdots \overset{k}{\rightleftarrows} S_n,$$

where S_i represents the ith site and k represents the rate of jumping between sites, and the arc angle between consecutive sites is denoted by θ_{ij}. A six-site model was used almost exclusively in simulations of helix motion in the aligned spectra primarily to minimize computational time, but simulations for larger N were investigated with only minor variation in line shape. In simulations of the motionally averaged line shapes of the oriented phase the rate of the helix six site jump is variable, with k ranging from $10^6\ s^{-1}$ and faster. The line shape changes observed for this range of k required only minor variation in P and σ to fit experimental spectra. If echo attenuation as a function of pulse spacing is simulated and scaled to the apparent $\langle T_{2e} \rangle$ of the dry sample, the rate of helix motion must be approximately $10^6\ s^{-1}$ to obtain simulations that produced the correct $\langle T_{2e} \rangle$ values. Calculated $\langle T_{2e} \rangle$ values obtained in this manner are presented in Tables I and II.

If only azimuthal helix motion is considered the line shape for 92% RH (W = 26.6) is simulated assuming $k = 10^6\ s^{-1}$, $\theta_{ij} = 60°$, $P = 0.7$, $\sigma = 15°$, $QCC_{\text{eff}} = 37.5$ kHz, and $\eta_{\text{eff}} \sim 0$. The effective quadrupole coupling constant can be obtained by use of the motional model presented for the unoriented studies,[29] consisting of a rapid threefold jump about a C_3 symmetry axis of the methyl group, and an additional fourfold libration of this C_3 axis in two perpendicular planes where θ_0 and ϕ_0 describe the angles of libration. Using the static QCC of 159 kHz as determined from the monomer studies[26] and a methyl angle of 70.5°, the librational angles θ_0 and ϕ_0 are found to equal approximately 25°. The experimental line shape for W = 29.6 is simulated similarly assuming $P \sim 1.0$, $\sigma = 15°$, $QCC_{\text{eff}} = 35.0$ kHz, and $\eta_{\text{eff}} \sim 0$ corresponding to librational angles of approximately 28°. Simulation of 95% RH (W = 39.8) is obtained with $k = 10^6\ s^{-1}$, $\theta_{ij} = 60°$ assuming $P \sim 1.0$, $\sigma = 20°$, $QCC_{\text{eff}} = 29.0$ kHz, and $\eta_{\text{eff}} \sim 0$, with θ_0 and ϕ_0 increasing to 32°. With increasing hydration there is an apparent reduction in the quantity of unoriented domains and a slight increase in the standard deviation of the Gaussian distribution. The determination of P and σ for room temperature spectra is complicated by the central isotropic resonance and are therefore only approximate values, but improved determination of σ may be obtained from the cylindrical line shape at lower temperatures.

In the previous investigation of the unoriented sample[29] it was noted that at high hydration levels the experimental line shapes become difficult to analyze due to local internal librations being masked by larger amplitude motions. In the

This article is copyrighted as indicated in the article. Reuse of AIP content is subject to the terms at: http://scitation.aip.org/termsconditions. Downloaded to IP: 199.212.66.33 On: Thu, 27 Nov 2014 12:31:48

analysis of the oriented phase, we have assumed that the dodecamer helix undergoes motion about its long axis. Contributions about an axis other than the azimuthal axis may need to be considered, since use of expressions for the rotational dynamics of circular cylinders applicable to shorter DNA fragments[37,38] show that the ratio of azimuthal to perpendicular diffusion is approximately 1.9 for a molecule with an approximately 1.7 length to diameter ratio. As a rough approximation to contributions for motion about an axis perpendicular to the helix axis the six-site jump motion about the helix axis was combined with a "helix wobble" described by a four-sites placed on a cone θ'_{ij} from the helix axis. If the internal librations are maintained at those observed for 88% RH (where the onset of helix motion is beginning to average the experimental line shape), a six-site jump motion about the helix axis and a helix wobble of $\theta'_{ij} \sim 10°$ simulates the line shape for 92% RH, while a wobble of $\theta'_{ij} \sim 15°$ reproduces the 95% RH line shape, with the values of P and σ remaining unchanged. Simulation of RI with variation of humidity was not pursued due to the numerous experimental conditions contributing to echo attenuation.

Line shape variation as a function of temperature for $W = 29.6$ also allows investigation of the rate and type of motion occurring within the sample. Elevation of the temperature to 309 K can be simulated by using the six-site jump motional model for helix motion increasing the rate to $k = 2.5 \times 10^6\ s^{-1}$, $\theta_{ij} = 60°$ assuming $P \sim 1.0$, $\sigma = 15°$, $QCC_{eff} = 32.0$ kHz, and $\eta_{eff} \sim 0$ corresponding to librational angles of approximately 30° [Fig. 2(a)]. The line shape for 295 and 286 K were simulated using the same model as discussed for 92% RH ($W = 29.6$) [Fig. 2(b)]. Lowering of the temperature results in broadening of the line shape as expected for motions approaching the intermediate regime, and can be simulated by reduction in the rate of helix motion as is seen on going from 276 K where $k = 8 \times 10^5\ s^{-1}$, with $QCC_{eff} = 37.5$ kHz, to 254 K with $k = 7 \times 10^5\ s^{-1}$ with $QCC_{eff} = 41.0$ kHz [Fig. 2(c)], to finally at 228 K with $k \approx 1 \times 10^2\ s^{-1}$, with $QCC_{eff} = 53.0$ kHz. While the majority of the spectra can be simulated using a single rate, the experimental line shape observed at 244 K requires a mixture of rates ranging from $k = 1 \times 10^2$ to $1 \times 10^5\ s^{-1}$.

Simulation of RI and $\langle T_{2e} \rangle$ using this simple six-site jump about a single axis fits the observed experimental values surprisingly well with the exception of RI at 309 K. With increasing temperature the apparent reduction in QCC_{eff} required to maintain the correct line shape assuming only motion about the helix axis can be explained by different mechanisms. If all these variation in QCC_{eff} are the result of reduction in the local fourfold libration with decreasing temperature, the angle of libration goes from θ_0 and $\phi_0 \sim 30°$ at 309 K to $\theta_0 \sim 10°$ and $\phi_0 \sim 15°$ at 228 K. As discussed earlier these line shape variations may also be the result of motions about the axis perpendicular to the long helix axis, and these temperature variations in line shape reflect changes in contributions from these motions. At 228 K helix motions are eliminated (at least on the time scale of ^2H NMR, which is on the order of kHz) giving rise to the highly characteristic cylindrical line shape. This line shape has been observed in a wide range of oriented samples, including ^2H labeled DNA fibers.[31,35] As seen in Fig. 3, the cylindrical line shape allows an excellent means to determine σ and P. Initial attempts to fit the line shape at 228 K with the distribution parameters observed at 295 K were unsuccessful. In particular, while the splitting of the perpendicular peaks and parallel shoulders were correctly simulated, the relative intensity of the shoulders with respect to the rest of the spectrum was poorly simulated. Variation in line shape due to anisotropic effects of slow motion about the helix axis were investigated but did not improve the fit of the parallel shoulders. This distortion has been noted previously,[31] and was attributed to orientationally dependent transverse relaxation. While this may indeed explain the observed distortion it was also found that variation in the oriented fraction P has a dramatic effect on the relative intensity of the shoulders. [See Fig. 3(b).] Simulations of the experimental spectra at 228 K with good agreement [Fig. 2(d)] were obtained if P decreased from ~ 1.0 to 0.7. If the presence of random domains also explains similar line shapes observed by Brandes and co-workers in oriented DNA fibers is unclear, but evidence of disordered regions has been studied by the same group.[39] This apparent increase in the disorder of the liquid crystal phase may result from changes in the liquid crystal domains with reduction in temperature or the difficulty of accurately determining P in the motionally averaged line shape at room temperature.

The effects of librational motion on the cylindrical line shape were also investigated. The resonant frequencies for an electrical field gradient tensor undergoing restricted diffusion in two perpendicular planes have been discussed for oriented films by Brandes and co-workers.[31] For a sample where the helix axis is aligned perpendicularly to the field ($\beta_0 = 90°$) and the time average angle between the base plane and the helix axis is perpendicular ($\langle \theta \rangle = 90°$) the resonant frequency is given by

$$\omega_Q = 3\pi/16 \left(\frac{e^2qQ}{h}\right)_{eff} \left\{ \left[1 - \eta - (3+\eta) \frac{\sin 2\theta_0}{2\theta_0} \right] - \cos 2\gamma \frac{\sin 2\phi_0}{2\phi_0} \left[3(1-\eta) + (3+\eta) \frac{\sin 2\theta_0}{2\theta_0} \right] \right\},$$

where $(e^2qQ/h)_{eff}$ is the effective quadrupole coupling constant as a result of the methyl rapid threefold jump, η is the asymmetry parameter (in this case an averaged asymmetry parameter which we assume to be zero due to the rapid methyl motion), γ is the angle of rotation of the C_3 symmetry axis about the DNA axis, θ_0 describes the extent of the tilt libration, and ϕ_0 describes the twisting libration. Therefore the perpendicular peaks or "horns" of the cylindrical line shape ($\gamma = 90°$) are not affected by a tilting libration, while the splitting between parallel edges ($\gamma = 0°$) is reduced by an increase in the tilt libration. In comparison, the twisting libration reduces both the horn and parallel edges splitting. These effects of librational motion on the quadrupolar spectral line shape are shown in Fig. 4.

Simulation of the cylindrical line shape for $W = 29.6$ at 228 K required the degree of librational motion to be $\theta_0 = 10° \pm 3°$ and $\phi_0 = 15° \pm 3°$, assuming the static value of (e^2qQ/h) is 159 kHz, and $\eta = 0$ as determined in monomer studies. These librational amplitudes are reduced from those

This article is copyrighted as indicated in the article. Reuse of AIP content is subject to the terms at: http://scitation.aip.org/termsconditions. Downloaded to IP: 199.212.66.33 On: Thu, 27 Nov 2014 12:31:48

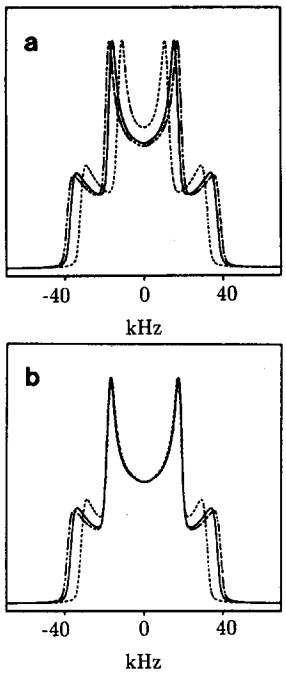

FIG. 4. Effects of librational amplitudes on simulated quadrupole echo spectrum. Spectrum obtained assuming $(e^2qQ/h) = 159$ kHz, $\eta = 0.0$, and a rapid methyl threefold jump in addition to variation in a four-site libration. (a) $\theta_0 = 0°$, (——) $\phi_0 = 5°$, (—) $\phi_0 = 10°$, (---) $\phi_0 = 20°$. (b) $\phi_0 = 0°$, (——) $\theta_0 = 5°$, (—) $\theta_0 = 10°$, (---) $\theta_0 = 20°$.

obtained from an analysis of the powder line shape at 88% RH. Temperature has been shown to have an effect on amplitude of librational motions within fibers,[31] but within the dodecamer these effects are complicated by motion about the helix axis. Temperature effects on libration can be more easily investigated at lower hydration levels where the motion about the helix axis is highly reduced. Experiments to obtain dry aligned samples from the liquid crystalline phase are now in progress. The tilting libration is larger than twisting-type librational motion for the dodecamer in an aligned phase, and is similar to that found in analysis of x-ray data on the same dodecamer.[40] The analysis of librational amplitudes (obtained from the effective asymmetry parameter assuming a four-site librational motion produced the observed asymmetry) as a function of hydration showed an anisotropic libration at lower humidities[29] for the methyl labeled dodecamer. If only librational averaging is considered the difference between the magnitude of θ_0 and ϕ_0 vanished with an increase in humidity. A similar trend was noted earlier in the analysis of librational amplitudes for oriented DNA fibers.[31] The analysis of the librational amplitudes in the oriented liquid crystal phase at reduced temperatures suggest that the reduction in the anisotropy of the libration with increasing hydration level may be the result of motion about the helix axis (leading to the symmetric line shape) not necessarily the magnitude of the tilting and twisting librations converging at elevated hydration levels. It may also be possible that these differences result from the librational angles θ_0 and ϕ_0 responding differently to reduction in temperature, but this requires additional investigation at reduced hydration levels. It should be noted that the mean angle of alignment β_0 also produces variation in the line shape [see Fig. 3(c)]. Large deviations from the assumption that the axis aligned perpendicular will produce line shapes where the splitting between parallel edges is reduced, thus affecting the determination of librational amplitude. This effect was not pursued further, and all simulations were obtained assuming $\beta_0 = 90°$.

It is also interesting to consider the effects of a nonmotionally induced asymmetry parameter of the methyl group on the line shape simulations. Hiyama *et al.* reported an *ab initio* MO study to explain the asymmetry parameter in thymine.[41] In the case of methyl group motion, a rapid threefold jump where the QCC is invariant between positions will produce an averaged EFG tensor that is axially symmetric regardless of the initial asymmetry parameter. Their calculations showed that the exocyclic oxygen of thymine produced an angular dependence on the quadrupole coupling constant with respect to the torsion angle describing the methyl group orientation. Starting with $\eta_{\text{static}} = 0.05$, averaging over a rapid threefold jump for a dihedral angle less than 20° produced the observed $\eta_{\text{eff}} = 0.07$ of thymine. If the effective values of the average methyl EFG tensor are used in the simulation of the aligned phase in [methyl ^{2}H]-2'-deoxythymidine labeled $[d(\text{CGCGAAT*T*CGCG})]_2$ ($QCC_{\text{eff}} = 51.5$ kHz, $\eta_{\text{eff}} = 0.06$) the experimental spectra could not be reproduced unless an additional tilting libration with a magnitude of $\theta_0 \sim 10°$ was included. The fact that motion still must be included to fit the line shape, in addition to a nonmotionally induced asymmetry parameter is further evidence that the model of motionally induced asymmetric line shapes is not unfounded.

We have reported short synthetic oligonucleotides spontaneously forming a liquid crystal-like phase at high hydration levels. Similar phase changes have been reported for larger fragments of DNA and RNA, but not for samples where the length to diameter ratio is approximately 1.7. Even though our data is not sufficient to evaluate existing theories concerning phase equilibria, a general comparison is in order. There have been theoretical treatments of asymmetric hard core fluids, including Flory's[42,43] lattice model of rod-like particles, Onsager,[44] and Lasher's[45] scaled particle treatment. All these theories predict critical volumes (critical concentration) being inversely proportional to the axial ratio. Calculation of the volume fraction is not straightforward for charged DNA molecules with a counter-ion atmosphere. The electrostatic repulsion of DNA can be accounted for by defining the hard-core radius in terms of the true radius augmented by a radius where the electrostatic potential is greater than $1/2k_BT$. Unfortunately all the theories are insufficient for small axial ratios. Flory's theory predicts a critical phase transitions only for axial ratios $(L/2a) \geqslant 2e \sim 5.4$, while the limiting ratio for Onsager's theory is approximately 4.0, and Lasher predicts the limiting ratio as low as 0.9.

Evaluating the synthetic oligonucleotide as spherocylinder with an effective radius a, length L, the volume fraction is given by[46]

$$\Phi = \rho V_{\text{eff}},$$

where ρ is the number density and the effective volume is given by

$$V_{\text{eff}} = 4\pi a^3/3 + \pi a^2 L.$$

This article is copyrighted as indicated in the article. Reuse of AIP content is subject to the terms at: http://scitation.aip.org/termsconditions. Downloaded to IP: 199.212.66.33 On: Thu, 27 Nov 2014 12:31:48

Volume fraction within the anisotropic phase were determined assuming $a \sim 12$ Å which is similar to the effective radius used by Brian *et al.*[46] for DNA at 2M NaCl. For $W = 26.6$ (722 mg ml^{-1}) the salt concentration corresponds to 1.25M NaCl, and the volume fraction was $\Phi \sim 1.5$, while for $W = 39.8$ (489 mg ml^{-1}) at 0.83 M NaCl, $\Phi \sim 1$. A volume fraction greater than unity suggests that the effective radius has been overestimated or that the oligonucleotide is not modelled well as a spherocylinder. To produce a volume fraction equal to unity by variation of the radius results in $a \sim 10$ Å at 722 mg ml^{-1} corresponding to an axial ratio of approximately two, and $a \sim 12$ Å at 489 mg ml^{-1}. These values of effective radius are significantly smaller than the 11.7 Å at 2 M NaCl and the 13 Å at 1 M NaCl reported by Brian *et al.*[46] Another possibility is the existence of end-to-end effects within the oligonucleotide sample. Volume fractions of unity calculated assuming a spherocylinder of length 2 L and radius a (two oligonucleotides end to end) still required $a = 10.7$ Å at 722 mg ml^{-1} and $a = 12.8$ Å at 489 mg ml^{-1}.

V. CONCLUSIONS

We have shown that at high hydration levels the [methyl ^{2}H]-2′-deoxythymidine labeled $[d(CGCGAAT*T*CGCG)]_2$ ^{2}H NMR spectra are simulated by assuming that the helix axis aligns perpendicular to the magnetic field with motion about the helix axis resulting in an averaging of the line shape. The rate of helix motion was monitored as a function of temperature and was observed to decrease from $k \sim 2.5 \times 10^6$ s^{-1} at 309 K to $k \sim 2 \times 10^5$ s^{-1} at 254 K until at 228 K a cylindrical line shape was observed ($k \sim 1 \times 10^2$ s^{-1}).

The degree of orientation is dependent on hydration level, but independent of magnetic field strength within the range investigated. Analysis of twisting and tilting type librational motion within the oriented phase at reduced temperature found $\theta_0 = 10° \pm 3°$ and $\phi_0 = 15° \pm 3°$ at 228 K. This anisotropic degree of libration contrasted to similar librational amplitudes obtained from simple analysis of the effective asymmetry parameter, η_{eff} in hydrated samples, and results from averaging due to motion about the helix axis. Attempts to obtain dry oriented samples of the dodecamer, in addition to careful analysis of relaxation behavior as a function of field strength are in progress. We are also pursuing similar investigations into the internal dynamics within the backbone of DNA utilizing dodecamers labeled at the 5′ and 5″ positions.

ACKNOWLEDGMENTS

We would like to thank Dr. Paul Ellis, Dr. Regitze Vold, and Dr. Robert Vold for providing original copies of the simulation program MXQET. This work was supported by a grant from the NSF (DMR-8700081), a NIH program project grant (GM-32681-06), and a NIH Molecular Biophysics grant to T.M.A. (Grant GM 08268-02).

[1] C. Robinson, Tetrahedron **13**, 219 (1961).
[2] V. Luzzati, A. Nicolaieff, and F. Masson, J. Mol. Biol. **3**, 185 (1961).
[3] E. Iizuka, Polym. J. **9**, 173 (1977).
[4] E. Iizuka, Polym. J. **10**, 235 (1978).
[5] E. Iizuka, Polym. J. **10**, 293 (1978).
[6] E. Iizuka and J. T. Yang, Liq. Cryst. Ordered Fluids **3**, 197 (1978).
[7] E. Iizuka and Y. Kondo, Mol. Cryst. Liq. Cryst. **51**, 285 (1979).
[8] E. Iizuka, Polym. J. **15**, 525 (1983).
[9] S. Skuridin, N. Badaev, A. Dembo, G. Lortkipanidze, and Yu. Yevdokimov, Liquid Crystals **3**, 51 (1988).
[10] R. L. Rill, P. R. Hillard, and G. C. Levy, J. Biol. Chem. **258**, 250 (1983).
[11] R. L. Rill, Proc. Natl. Acad. Sci. USA **83**, 342 (1986).
[12] T. E. Strzelecka and R. L. Rill, J. Am. Chem. Soc. **109**, 4513 (1987).
[13] T. E. Strzelecka, M. W. Davidson, and R. L. Rill, Nature **331**, 457 (1988).
[14] R. Brandes and D. R. Kearns, Biochemistry **25**, 5890 (1986).
[15] G. P. Spada, A. Carcuro, F. Colonna, A. Garbesi, and G. Gottarelli, Liquid Crystals **3**, 651 (1988).
[16] P. Mariani, C. Mazabard, A. Garbesi, and G. P. Spada, J. Am. Chem. Soc. **111**, 6369 (1989).
[17] A. Baram and Z. Luz, J. Chem. Phys. **64**, 4321 (1976).
[18] Z. Luz, R. Poupko, and E. T. Samulski, J. Chem. Phys. **74**, 5825 (1981).
[19] R. Poupko, Z. Luz, N. Spielberg, and H. Zimmermann, J. Am. Chem. Soc. **111**, 6094 (1989).
[20] J. H. Freed, G. V. Bruno, and C. F. Polnaszek, J. Phys. Chem. **75**, 3385 (1971).
[21] R. F. Campbell, E. Meirovitch, and J. H. Freed, J. Phys. Chem. **83**, 525 (1979).
[22] L. J. Schwartz, E. Meirovitch, J. A. Ripmeester, and J. H. Freed, J. Phys. Chem. **87**, 4453 (1983).
[23] M. Mehring, *Principles of High Resolution NMR in Solids* (Springer, Berlin, 1983).
[24] M. S. Greenfield, A. D. Ronemus, R. L. Vold, and R. R. Vold, J. Magn. Reson. **72**, 89 (1987).
[25] R. J. Wittebort, E. T. Olejniczak, and R. G. Griffin, J. Chem. Phys. **86**, 5411 (1987).
[26] A. Kintanar, T. M. Alam, W.-C. Huang, D. C. Schindele, D. E. Wemmer, and G. Drobny, J. Am. Chem. Soc. **110**, 6367 (1988).
[27] J. Gladden and G. Drobny (unpublished results).
[28] R. G. Griffin, Methods Enzymol. **72**, 108 (1981).
[29] T. M. Alam and G. Drobny, Biochemistry (submitted).
[30] R. C. Weast, *Handbook of Chemistry and Physics*, 60th ed. (CRC, Boca Raton, FL, 1979), p. E-46.
[31] R. Brandes, R. R. Vold, D. R. Kearns, and A. Rupprecht, J. Mol. Biol. **202**, 321 (1988).
[32] R. E. Dickerson and H. R. Drew, J. Mol. Biol. **149**, 761 (1981).
[33] W. Nerdal, D. R. Hare, and B. R. Reid, Biochemistry (submitted).
[34] T. Fujiwara and H. Shindo, Biochemistry **24**, 896 (1985).
[35] H. Shindo, Y. Hiyama, S. Roy, J. S. Cohen, and D. A. Torchia, Bull. Chem. Soc. Jpn. **60**, 1631 (1987).
[36] A. Kintanar, W.-C. Huang, D. C. Schindele, D. E. Wemmer, and G. Drobny, Biochemistry **28**, 282 (1989).
[37] M. M. Tirado and J. García de la Torre, J. Chem. Phys. **73**, 1986 (1980).
[38] M. M. Tirado, C. Martinez, and J. García de la Torre, J. Chem. Phys. **81**, 2047 (1984).
[39] R. Brandes, R. R. Vold, D. R. Kearns, and A. Rupprecht, Biopolymers **27**, 1159 (1988).
[40] S. R. Holbrook and S.-H. Kim, J. Mol. Biol. **173**, 361 (1984).
[41] Y. Hiyama, S. Roy, K. Guo, L. G. Butler, and D. A. Torchia, J. Am. Chem. Soc. **109**, 2525 (1987).
[42] P. J. Flory, Proc. R. Soc. London, Ser. A **234**, 60 (1956).
[43] P. J. Flory, Proc. R. Soc. London, Ser. A **234**, 73 (1956).
[44] L. Onsanger, Ann. N. Y. Acad. Sci. **51**, 627 (1949).
[45] G. Lasher, J. Chem. Phys. **53**, 4141 (1970).
[46] A. A. Brian, H. L. Frisch, and L. S. Lerman, Biopolymers **20**, 1305 (1981).

This article is copyrighted as indicated in the article. Reuse of AIP content is subject to the terms at: http://scitation.aip.org/termsconditions. Downloaded to IP: 199.212.66.33 On: Thu, 27 Nov 2014 12:31:48